Precipitation of γ' during cooling of nickel-base superalloy Haynes 282

N.B. When citing this work, cite the original published paper.

(article starts on next page)
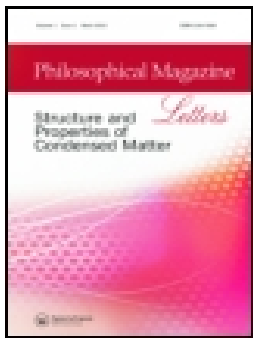
Precipitation of γ during cooling of nickel-base superalloy Haynes 282

Ceena Joseph , Mattias Thuvander , Christer Persson & Magnus Hörnqvist Colliander

Published online: 04 Nov 2020.

Submit your article to this journal ⧉

Article views: 88

View related articles ⧉

View Crossmark data ⧉

Taylor & Francis
Taylor & Francis Group

🔓 OPEN ACCESS | Check for updates

Precipitation of γ′ during cooling of nickel-base superalloy Haynes 282

Ceena Joseph[a]*, Mattias Thuvander[b], Christer Persson[a] and Magnus Hörnqvist Colliander[b]

[a]Department of Industrial and Materials Science, Chalmers University of Technology, Göteborg, Sweden; [b]Department of Physics, Chalmers University of Technology, Göteborg, Sweden

ABSTRACT

Cooling-induced precipitation of the strengthening γ′ phase is commonly investigated in Ni-base superalloys with a high γ′ volume fraction, where it is used to control the final microstructure and properties. Less is known about the phase separation in low-volume-fraction alloys during cooling, although the microstructural state after cooling from solution treatment is known to affect subsequent heat-treatment steps. We use atomic-scale characterisation of Ni-base superalloy Haynes 282 (equilibrium γ′ volume fraction around 20%) to show that air cooling after solution or carbide stabilisation results in precipitation of nm-sized γ′ particles, whereas precipitation was suppressed during water quenching. The solution treatment has a significant effect on the hardness and γ′ precipitation during air cooling from the subsequent carbide stabilisation temperature. Also, the carbide-stabilisation treatment itself affects the γ′ precipitation during subsequent air cooling.

Introduction

Precipitation-strengthened nickel-base superalloys have been developed to meet the ever-increasing demand for higher operating temperatures in gas turbines used in aircraft and power-generation units [1–3]. One such recently developed nickel-base superalloy, Haynes 282, has been attracting interest owing to a combination of properties such as creep strength, thermal stability and fabricability [4]. A good combination of these properties is achieved on account of the precipitation of a strengthening phase (γ′, L1$_2$ Ni$_3$(Al,Ti)) and grain-boundary carbides (mainly M$_{23}$C$_6$ and M$_6$C) during heat treatment [1]. To adequately determine the influence of microstructure on high-temperature

performance, it is critical to understand the nature of precipitation during and after heat treatment.

An earlier heat-treatment study on Haynes 282 sheet material showed that directly applying a standard two-step heat treatment (1010°C/2 h + 788°C/ 8 h) to mill-annealed material, without initial solution treatment, resulted in an increase in both strength and ductility as compared to the solutionized (at 1120°C) and heat-treated condition [5]. One observation from that study, which was left unexplained, was the difference in hardness measured after quenching from the carbide stabilisation treatment (2 h at 1010°C; first step in the two-step ageing treatment) of mill-annealed and solution-treated material. The present contribution is aimed at further probing the effect of solution treatment, and in particular the cooling rate, on the subsequent behaviour during carbide stabilisation by detailed characterisation of the precipitation state after different heat treatments using atom probe tomography (APT), a technique that enables atomic-level microstructural characterisation [6,7].

The hardness of Ni-base superalloys is controlled by the precipitation of γ', which exhibits fast enough kinetics to allow nucleation during cooling after solution treatment. The majority of the published studies regarding cooling-induced precipitation in Ni-based superalloys have been focused on high-volume-fraction (typically powder-metallurgy) alloys, in which precipitation readily occurs even during fast cooling from solution treatment, see for example [6–15]. Information regarding precipitation during cooling of relatively low-volume-fraction alloys, on the other hand, is scarce in the literature, especially for high cooling rates. In Alloy 718, no (or very limited) precipitation of γ' and/or γ'' could be seen in transmission electron microscopy (TEM) micrographs following air cooling or water quenching from solution treatments at 1045°C/45 min, whereas furnace cooling resulted in significant precipitation of γ', γ'' and δ [13]. For Haynes 282, γ' particles in the size range 10–20 nm have been reported in thicker solution-treated sections owing to the slow cooling [16]. Fahrmann and Pike [17] also reported indications of small (< 10 nm in diameter) γ' in high-resolution scanning electron microscopy (SEM) images of mill-annealed thin sheet (1.6 mm thick, mill-annealed at 1149°C), which was consistent with previous experiments and simulations using controlled cooling rates [18]. No such indications were found in the previous study of 3 mm sheet used in this investigation [5], which could arise from differences in processing history. However, the exact history of the previously investigated 3 mm sheet was not available for comparison. Polkowska et al. [19] also suggested that the studied 1.6 mm thick sheet in the mill-annealed condition could contain γ' particles below the resolution limit of SEM based on the heat-treatment response when aged below the carbide solvus temperature. Similarly, slow cooling from solution treatment at 1135°C led to coarser γ' particles after one-step aging at 800°C (without carbide stabilisation) of a 15 mm

thick plate [20], indicating the presence of cooling-induced nucleation after solutionizing.

In order to address the issue of γ' formation during cooling in Haynes 282 we investigate the presence of nanoscale precipitation in the mill-annealed condition and compare this with the microstructure obtained after solution treatments followed by cooling at different rates. Furthermore, we study the precipitation state after a carbide-stabilisation treatment of material in different starting states, and cooled at different rates, in order to further understand the effect of the initial solution treatment on the precipitation during the subsequent heat-treatment step.

Materials and methods

The material used in this study was a 3 mm thick sheet (the same as used in [5]), received in the mill-annealed state. The exact conditions for the mill-annealing are not known, but it was manufactured as per specification AMS5951. The nominal composition (in wt.%) is Ni-19.5Cr-10.1Co-8.67Mo-2.24Ti-1.48Al-1.0Fe-0.053C-0.05Si-0.005B-0.002P-0.002S. The average grain size was measured to be 150 μm, and primary MC carbides were sparsely dispersed inter- and intra-granularly. Samples with dimensions of $20 \times 20 \times 3 \ mm^3$ were cut from the sheet by water-jet cutting and heat treatments were performed in a box furnace in air. The different heat treatments are summarised in Table 1. Three different starting conditions were investigated: the mill-annealed state and two states subjected to solution treatment at 1120°C for 30 min followed by air cooling or water quenching. The duration of the solution treatments was chosen to achieve complete dissolution of secondary carbides without inducing noticeable grain growth [21]. Specimens from all starting conditions were subjected to a subsequent carbide stabilisation treatment at 1010°C for 2 h, followed by air-cooling or water-quenching.

The temperature histories obtained during air-cooling from 1120 and 1010°C were measured using spot-welded thermocouples on dummy specimens. The resulting temperature and cooling rates are shown in Figure 1. A typical time to reach a temperature of around 500°C, where diffusion is negligible, is around 1 min when starting from 1010°C (corresponding to an average

Table 1. Summary of the applied heat treatments. Note: solution treatment (ST): 1120°C/30 min, stabilisation treatment: 1010°C/2 h.

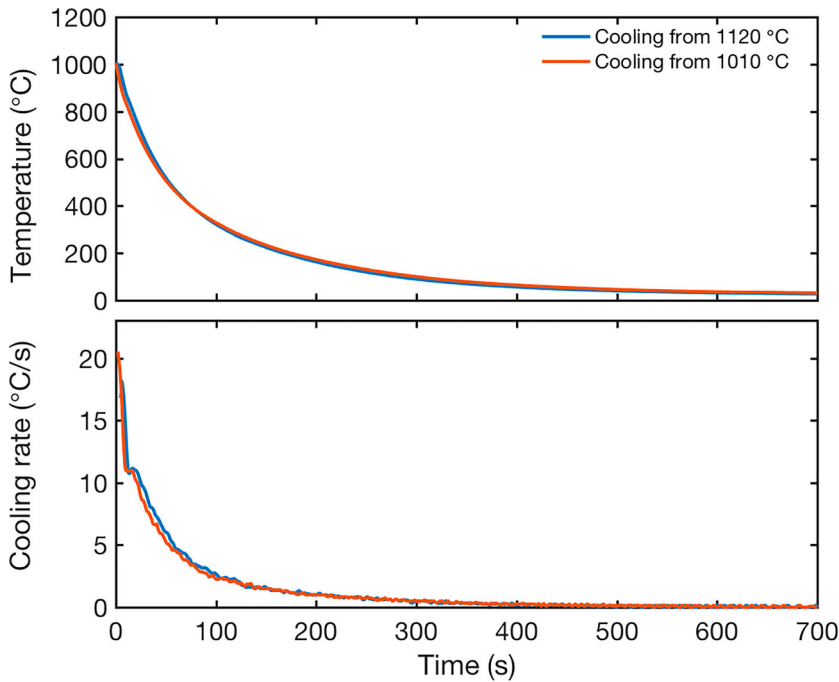| Starting condition	Cooling from stabilisation treatment	Designation
Mill-annealed (MA)	Air-cooled (AC)	MA + 1010/AC
	Water-quenched (WQ)	MA + 1010/WQ
Solution-treated (ST) and air-cooled (AC)	Air-cooled (AC)	ST/AC + 1010/AC
	Water-quenched (WQ)	ST/AC + 1010/WQ
Solution-treated (ST) and water-quenched (WQ)	Air-cooled (AC)	ST/WQ + 1010/AC
	Water-quenched (WQ)	ST/WQ + 1010/WQ

Figure 1. Temperature and cooling rate as a function of time when cooling from 1120°C and 1010°C, respectively, in air. For cooling from 1120°C only the part below 1010°C is shown.

cooling rate of around 10°C s^{-1}), and finite-element (FE) simulations showed that the temperature gradient between the centre of the specimen and the surface, where the thermocouple is placed, was negligible. The cooling curves in the range 1010°C–500°C are virtually identical, independent of the starting temperature (1120 or 1010°C). The cooling rate during water-quenching was not measured but was certainly at least an order of magnitude higher.

All nine conditions were characterised by SEM (LEO Gemini 1550), hardness measurement and APT. Standard metallographically prepared specimens were etched with γ′ etchant (15 g CrO$_3$, 150 ml H$_3$PO$_4$, 10 mL H$_2$SO$_4$) to reveal the features in SEM. Hardness testing was performed according to ASTM standard E92 and a Vickers macro-hardness with 10 kg load. An average of five measurements is reported in this study. APT samples were prepared by producing 10 mm long blanks with square cross-section of typical dimensions 0.2×0.2 mm^2. The blanks were cut out of the bulk material using a water-cooled diamond cutting blade. Needle-shape specimens were produced from the blanks by electropolishing using standard solutions and conditions for nickel alloys (10% perchloric acid and 20% glycerol in methanol and 2% perchloric acid in 2-butoxyethanol). The material was characterised using an atom probe instrument LEAP 3000X HR, from Imago Scientific Instruments, using a specimen temperature of 30 K, a laser pulse energy of 0.30 nJ at a wavelength of 532 nm and a pulse repetition rate of 200 kHz.

Particles were identified based on Al iso-concentration surfaces (threshold 12 at.%, voxel size 1 nm^3 and delocalisation $3 \times 3 \times 1.5$ nm^3), and volume fractions were calculated as the fraction of atoms contained in the identified particles divided by the total number of atoms in the reconstructed volumes. Number densities were calculated as the sum of the number of particles fully contained in the analysed volume and half the number of particles on the volume edge, divided by the total analysed volume (which in turn was calculated from the total number of atoms in the analysis, the detection efficiency (37%) and the lattice parameter for Haynes 282).

Results and discussion

Results from the SEM investigation are shown in Figure 2. A small amount of grain-boundary carbides is seen in the mill-annealed state, which are dissolved during solutionizing. The carbide stabilisation treatment produces a distribution of discrete carbide particles in grain boundaries, as expected. No precipitation of γ' is seen in the grain boundaries, and in no case was intragranular γ' observed in the SEM.

The hardness of the heat-treated specimens is shown in Figure 3. As previously observed [5], the hardness decreased from the mill-annealed state after solution treatment and water quenching. In contrast, an increase in
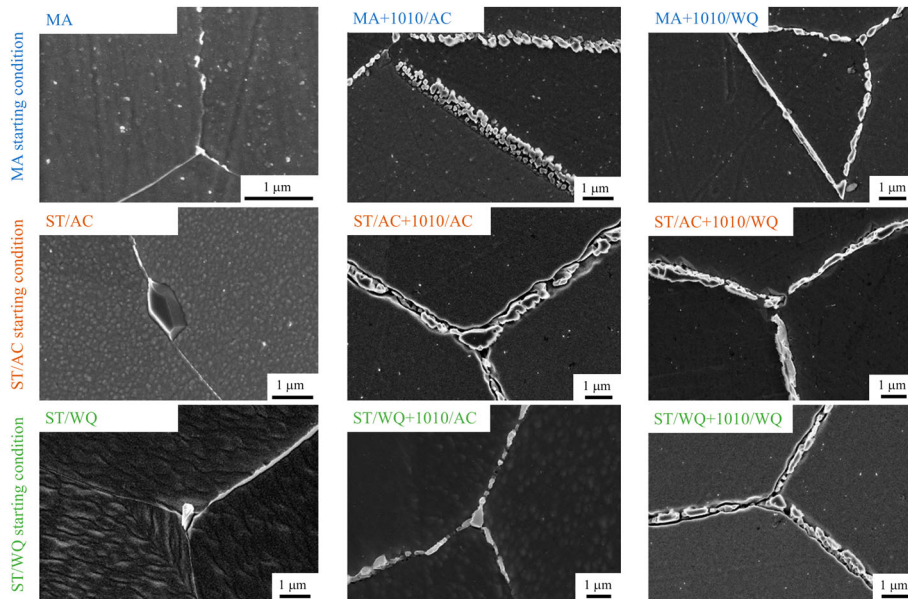

Figure 2. SEM images showing the presence of grain-boundary carbides and the absence of large γ' precipitates with different heat-treatment conditions revealed by oxalic-acid etching. Note that particle-like features in the grain interiors (most clearly visible in the ST/AC and ST/WQ + 1010/AC conditions) are artefacts from electrolytic etching, and not γ'.
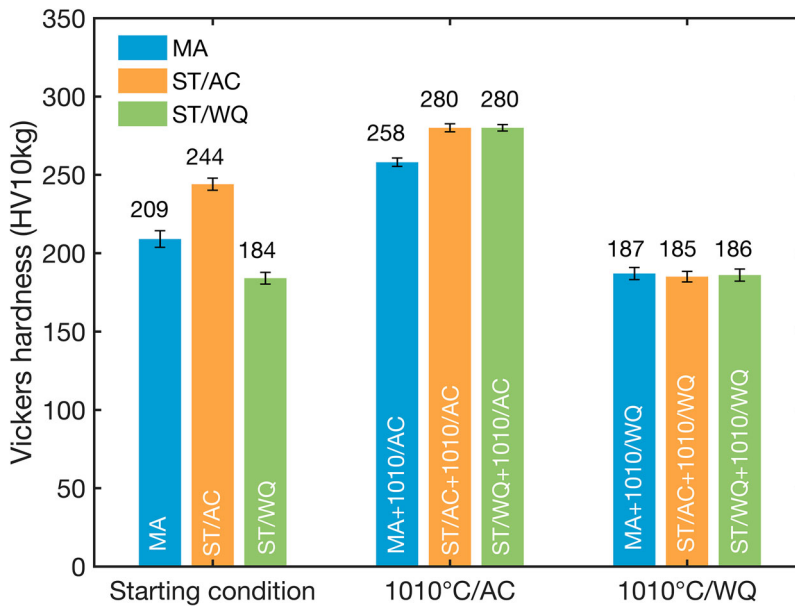
Figure 3. Hardness after different heat treatments.

hardness is observed after air-cooling from the solutionizing temperature. As no grain growth occurred during the solution treatment, these observations suggest that dissolution of precipitates induced by cooling in the mill-annealed state is responsible for the decrease in hardness after solution treatment and water quenching, and that the precipitation process is fast enough to result in significant phase separation during air cooling, but not during water quenching. The higher hardness in the solution-treated and air-cooled samples compared to the mill-annealed condition further indicates that the cooling rate during mill annealing was relatively rapid, presumably faster than the current air-cooling.

Water quenching from the carbide-stabilisation-treatment temperatures results in the same hardness, independent of starting condition, corresponding to the hardness level observed after solution treatment and water quenching. This suggests that all prior cooling-induced γ' is dissolved at 1010°C. It also confirms that the grain-boundary carbides (which are present after the stabilisation treatment but not after solution treatment) have negligible influence on the hardness level. Air cooling from 1010°C, on the other hand, results in significant differences between the mill-annealed and the solution-treated starting condition, where specimens subjected to an initial solution treatment show around 20 HV (8.5%) higher hardness. As the specimens showed very similar hardness after water quenching from carbide stabilisation, this difference must arise from differences in precipitation during cooling and indicates that this process is affected by the prior solution treatment. Surprisingly, the effect observed here is opposite to that seen in the previous study, where

mill-annealed specimens showed higher hardness (equal to that observed in the mill-annealed starting state) than solution-treated specimens after carbide stabilisation and quenching. One possible reason is that the grain growth occurring during the longer solution-treatment times used in [5] also reduced the dislocation density and thus the number of potential nucleation sites, but this clearly requires further studies. Furthermore, the hardness obtained after air cooling the solution-treated materials from the carbide stabilisation treatment showed some 35 HV (∼14%) higher hardness compared to those air cooled from the solutionizing temperature. As the temperature history in the region where γ' precipitation is expected to occur is virtually identical in the two cases (see Figure 1), this indicates that, besides the effect of the initial solution treatment, the 2 h spent at 1010°C also alters the subsequent precipitation behaviour.

The presence of γ' in the mill-annealed state was confirmed by APT (Figure 4 and Table 2). Water quenching after solution treatment resulted in the complete absence of γ', confirming the reason for the strength difference suggested above, whereas air cooling produced a precipitation state qualitatively similar to the mill-annealed condition (Figure 4). The average γ' size was the same in these two conditions (diameter 2.5 nm), whereas the number density is higher in the air-cooled solution-treated specimen, which is consistent with the higher hardness.

As in the solution-treated and water-quenched material, no γ' was found in specimens that were water quenched from 1010°C. Air cooling from 1010°C, on the other hand, results in precipitation of γ', consistent with the increased hardness of these materials. The size and number density of the γ' found after air cooling from the carbide-stabilisation treatment of the two solution-treated starting conditions are very similar. As the absence of γ' after carbide
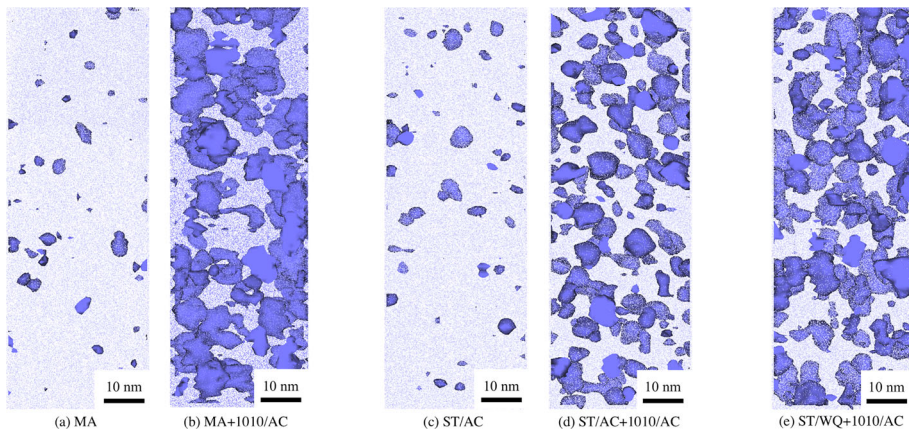

Figure 4. Atom probe tomography reconstructions of the different material conditions where γ′ precipitation could be detected. 12 at.% Al iso-concentration surface is used to visualise the γ/γ′ interfaces, with Cr atoms in light blue. The slice thickness is 35 nm.

Table 2. Results of APT analysis showing the size (average diameter), number density and volume fraction of γ′ precipitates.

Heat treatment	Hardness (HV)	Size (nm)	Number density (10^{-3} nm^{-3})	Volume fraction (%)
MA	209	2.5	0.17	0.2
MA + 1010 /AC	258	6.0	0.43	7.3
MA + 1010/WQ	187	–	–	–
ST/AC	244	2.5	0.33	0.3
ST/AC + 1010/AC	280	3.9	1.1	5.8
ST/AC + 1010/WQ	185	–	–	–
ST /WQ	184	–	–	–
ST /WQ + 1010/AC	280	4.2	1.2	5.8
ST /WQ + 1010/WQ	186	–	–	–

stabilisation and water quenching indicates that the particles were completely dissolved at 1010°C, and the temperature histories during air-cooling from 1120 and 1010°C were almost identical below the carbide stabilisation temperature (Figure 2), one would expect the precipitation state to be very similar after air cooling from the two temperatures. However, the hardness measurements reported above indicate otherwise. Compared to the solution-treated and air-cooled state, the particle size after the 1010°C treatment is larger (∼ 4 nm compared to 2.5 nm) and the number density is higher by a factor of 3–4. The carbide stabilisation step applied after solution treatment clearly has a pronounced effect on the γ′ precipitation during the subsequent cooling. This effect is not related to the γ′ precipitated during the cooling from the initial solution treatment, as indicated by the similarity in the γ′ size and number density after air cooling of the two solution treated conditions from 1010°C, which again is consistent with the complete dissolution of γ′ at this temperature, as shown above. These results are entirely consistent with the observations made from the hardness measurements. As the cooling-induced precipitation will depend on the distribution of the chemical elements in the matrix, several different explanations for the effect of the carbide stabilisation on the subsequent precipitation can be considered. Homogenisation during the carbide stabilisation might play a role, but this effect should be minor in samples subjected to prior solution treatment. Furthermore, during the stabilisation treatment, the primary carbides, rich in Ti, can partially decompose according to MC→$M_{23}C_6$/M_6C + γ. Since $M_{23}C_6$ does not contain Ti [16], and M_6C only dissolves small amounts of Ti (around 2–3 at.% [16]), it is possible that the increased Ti content released during decomposition can, at least locally, promote γ′ precipitation. The formation of secondary carbides will also bind Cr and Mo from the matrix in the carbides, thereby effectively enriching the matrix in γ′ forming elements. The dominating mechanism can, however, not be concluded from the present study.

Interestingly, further differences are seen when comparing with the microstructure observed after carbide stabilisation and air cooling of the mill-annealed starting condition. Here, the γ′ size is even larger (around 6 nm in

diameter), but the number density is close to that observed in the mill-annealed or solution-treated and air-cooled condition. This significant difference from that observed after the 1010°C treatment of the solution-treated starting condition directly confirms the pronounced effect of solutionizing on subsequent heat treatments, as previously observed from the hardness measurements. While the detailed mechanisms behind this effect cannot be resolved from the present investigation, it is likely that the homogenisation of the matrix during solution treatment plays an important role for the response during subsequent steps.

Conclusions

In summary, a detailed characterisation of Haynes 282 after different heat treatments has revealed the following:

(1) The mill-annealed (as-received) state contained nano-scale γ' precipitates. The dissolution of these precipitates at 1120°C is responsible for the previously observed drop in hardness after solutionizing and water-quenching.
(2) Whereas water-quenching suppresses precipitation after solutionizing, air-cooling at an average rate corresponding to ∼10°C/s to 500°C, results in a state similar to the mill-annealed.
(3) The solution treatment also affects the precipitation during cooling from a subsequent carbide-stabilisation treatment at 1010°C, as seen from differences in the hardness and γ' distribution after carbide stabilisation and cooling, when starting from the mill-annealed or the solution-treated condition.
(4) The carbide precipitation treatment itself also affects the precipitation process, giving a different hardness and precipitate structure than after initial solutionizing, in spite of the virtually identical temperature history during cooling. Hardness measurements and APT observations were consistent throughout.

Acknowledgements

Disclosure statement

Funding

References

[1] R.C. Reed, *The Superalloys - Fundamentals and Applications*, Cambridge University Press, Cambridge, UK, 2008.

[2] R.F. Smith, G.J. Lewi and D.H. Yates, Aircraft Eng. Aero. Tech 73 (2001) pp.138–147.

[3] T.M. Pollock and S. Tin, J. Propul. Power 22 (2006) pp.361–374.

[4] L. Pike, Proc. 11th Int. Symp. on Superalloys, TMS (2008) pp.191–200.

[5] C. Joseph, C. Persson and M. Hörnqvist Colliander, Mater. Sci. Eng. A 697 (2017) pp.520–530.

[6] A.R.P. Singh, S. Nag, J.Y. Hwang, G.B. Viswanathan, J. Tiley, R. Srinivasan, H.L. Fraser and R. Banerjee, Mater. Char 62 (2011) pp.878–886.

[7] A.R.P. Singh, S. Nag, S. Chattopadhyay, Y. Ren, J. Tiley, G.B. Viswanathan, H.L. Fraser and R. Banerjee, Acta Mater. 61 (2013) pp.280–293.

[8] S.S. Babu, M.K. Miller, J.M. Vitek and S.A. David, Acta Mater. 49 (2001) pp.4149–4160.

[9] P. Le Baillif, P. Lamesle, D. Delagnes, V. Velay, C. Dumont and F. Rézai-Aria, MATEC Web of Conf 14 (2014) pp.21002.

[10] S.L. Semiatin, S.-L. Kim, F. Zhang and J.S. Tiley, Mater. Trans 46A (2015) pp.1715–1730.

[11] Y.Q. Chen, E. Francis, J. Robson, M. Preuss and S.J. Haigh, Acta Mater. 85 (2015) pp.199–206.

[12] X. Fan, Z. Guo, X. Wang, J. Yang and J. Zou, Mater. Char. 139 (2018) pp.382–389.

[13] D.-G. He, Y.C. Lin, Y. Tang, L. Li, J. Chen, M.-S. Chen and X.-M. Chen, Mater. Sci. Eng. A 746 (2019) pp.372–383.

[14] H. Huang, G. Liu, H. Wang, Z. Wang, H. Zhang, Y. Shao and B. Hu, J. Alloys Comp 805 (2019) pp.1254–1259.

[15] H. Huang, H. Zhang, B. Hu, H. Wang and G. Liu, Intermetallics 116 (2020) pp.106659.

[16] R. Viswanathan, J. Hawk, R. Schwant, D. Saha, T. Totemeier, S. Goodstine, M. McNally, D.B. Allen and R. Purgert, *Steam Turbine Materials for Ultrasupercritical Coal Power Plants. United States*, Technical Report, (2009).

[17] M.G. Fahrmann and L.M. Pike, Proc. 9th Int. Conf. on Superalloy 718 and Derivatives, TMS (2018) pp.565–579.

[18] M.G. Fahrmann and D.A. Metzler, JOM 68 (2016) pp.2786–2792.

[19] A. Polkowska, W. Polkowski, M. Warmuzek, N. Ciesta, G. Wloch, D. Zasada and R.M. Purgent, J. Mater. Eng. Perform 28 (2019) pp.3844–3851.

[20] K.-Y. Shin, J.-H. Kim, M. Terner, B.-O. Kong and H.-U. Hong, Mater. Sci. Eng. A 751 (2019) pp.311–322.

[21] S. Suhas, *Effect of solutionizing heat treatment on microstructure and properties of nickel based superalloy Haynes 282*, M.Sc. Thesis, Chalmers University of Technology, 2016.